HHS Public Access

Author manuscript

Prostaglandins Other Lipid Mediat. Author manuscript; available in PMC 2023 February 01.

Published in final edited form as:

Prostaglandins Other Lipid Mediat. 2022 February ; 158: 106605. doi:10.1016/j.prostaglandins.2021.106605.

Ca^{2+}-Independent Phospholipase $A_2\beta$-Derived PGE_2 Contributes to Osteogenesis

William D. Hancock[1,†], **Xiaoyong Lei**[2,3,†], **Gregory A. Clines**[4,†], **Ying G. Tusing**[2,3], **Susan E. Nozell**[5], **Sasanka Ramanadham**[2,3,*]

[1]Department of Biochemistry and Molecular Biology Virginia Commonwealth University, Richmond, VA, USA

[2]Department of Cell, Developmental, and Integrative Biology, University of Alabama at Birmingham, Birmingham, AL USA

[3]Comprehensive Diabetes Center, University of Alabama at Birmingham, Birmingham, AL USA

[4]Department of Internal Medicine, University of Michigan, Ann Arbor, MI

[5]Department of Radiation Oncology, University of Alabama at Birmingham, Birmingham, AL USA

Abstract

Bone modeling can be modulated by lipid signals such as arachidonic acid (AA) and its cyclooxygenase 2 (COX2) metabolite, prostaglandin E_2 (PGE_2), which are recognized mediators of optimal bone formation. Hydrolysis of AA from membrane glycerophospholipids is catalyzed by phospholipases A_2 (PLA_2s). We reported that mice deficient in the Ca^{2+}- independent PLA_2beta ($iPLA_2\beta$), encoded by *Pla2g6*, exhibit a low bone phenotype, but the cause for this remains to be identified. Here, we examined the mechanistic and molecular roles of $iPLA_2\beta$ in bone formation using bone marrow stromal cells and calvarial osteoblasts from WT and $iPLA_2\beta$-deficient mice, and the MC3T3-E1 osteoblast precursor cell line. Our data reveal that transcription of osteogenic factors (*Bmp2*, *Alpl*, and *Runx2*) and osteogenesis are decreased with $iPLA_2\beta$-deficiency. These outcomes are corroborated and recapitulated in WT cells treated with a selective inhibitor of $iPLA_2$ β (10 μM *S*-BEL), and rescued in $iPLA_2\beta$-deficient cells by additions of 10 μM PGE_2. Further, under osteogenic conditions we find that PGE_2 production

[*]**To whom correspondence should be addressed**: Dr. Sasanka Ramanadham, PhD, Professor, Department of Cell, Developmental, and Integrative Biology ***(CDIB)***, Senior Scientist, Comprehensive Diabetes Center, University of Alabama at Birmingham ***(UAB)***, Shelby Biomedical Research Building, Rm. 1205, Birmingham, AL 35294-2182, 205-996-5973 (off); 996-5220 (fax); sramvem@uab.edu.

[†]Contributed equally to the studies

Author contributions-WDH designed and performed experiments, analyzed data, prepared figures, and wrote the paper. XY performed PGE_2 assays, analyzed data, and edited the manuscript. GAC performed analyses in the MC3T3-E1 cells, advised on *in vitro* experiments, and edited the paper. SEN provided expertise with the ChIP analyses, analyzed data, and edited the paper. YGT bred and genotyped mice. SR conceived and coordinated the study, analyzed data, contributed to preparation of the figures, and edited the paper.

DISCLOSURES

The authors declare that they have no conflicts of interest with the contents of this article.

Declarations of Interest: None.

is through iPLA$_2$β activity and that this leads to induction of *Runx2* and *iPLA$_2$β* transcription. These findings reveal a strong link between osteogenesis and iPLA$_2$β-derived lipids and raise the intriguing possibility that iPLA$_2$β-derived PGE$_2$ participates in osteogenesis and in the regulation of Runx2 and also iPLA$_2$β.

Keywords

osteogenesis; lipid-signaling; PGE$_2$; iPLA$_2$β; Runx2

1. INTRODUCTION

Adult bone is remodeled continuously and the process of bone resorption must be balanced by the process of bone formation to maintain bone mass and preserve bone structure and strength. Loss in bone mass and strength occurs with aging and these can lead to increased incidence of fractures [1-7]. The overall bone phenotype with aging is a consequence of balance between the function of bone-forming osteoblasts and bone-resorbing osteoclasts [1-3,5-8].

Among the factors that influence bone formation are lipid signals generated via activation of phospholipases A$_2$ (PLA$_2$s) [9-12]. Numerous studies suggest that the downstream lipid products (i.e. leukotrienes, hydroxyeicosatetraenoic acids, platelet activating factor) of these PLA$_2$s predominantly enhance bone resorption [13-19]. In addition to cytosolic (c) and secretory (s) PLA$_2$s, osteoblasts express a Ca^{2+}-independent PLA$_2$beta (iPLA$_2$β) enzyme that is encoded by the *Pla2g6* gene [20]. The iPLA$_2$β participates in a variety of biological processes and we find that iPLA$_2$β-deficiency leads to decreased osteoblast function and age-related bone loss [20]. These findings suggest that iPLA$_2$β-derived lipids (iDLs) enhance bone formation.

As a member of the PLA$_2$ family, iPLA$_2$β catalyzes the hydrolysis of the *sn*-2 substituent from glycerophospholipid substrates to yield a free fatty acid (i.e. arachidonic acid, AA) and a 2-lysophospholipid [21]. Both AA and its cyclooxygenase metabolite, prostaglandin E$_2$ (PGE$_2$) are recognized to increase bone mineral density [22], bone mass [23,24], and decrease bone resorption [25]. It has been suggested that PGE$_2$, which in the bone is produced mainly by osteoblasts [26-29], is the main mediator of AA-induced bone formation via activation of the EP$_4$ receptor [26,30-33]. However, the molecular mechanisms by which iDLs impact bone formation are not well understood.

To delineate the role of iPLA$_2$β and iDLs on bone formation, we utilized bone marrow stromal cells (BMSCs), calvarial osteoblasts, and MC3T3-E1 osteoblast cells to assess osteogenic transcripts, proteins, mineralization, and molecular links. Here, we report the novel findings that (1) PGE$_2$ generated via iPLA$_2$β activation is critical for osteogenesis (2) reduced osteogenesis due to iPLA$_2$β-deficiency is rescued by PGE$_2$ supplementation, and (3) PGE$_2$-signaling through the EP$_4$ receptor induces not only Runx2, but also iPLA$_2$β during osteogenesis.

2. MATERIALS AND METHODS

2.1. Animals.

Breeders (*iPLA$_2\beta^{-/-}$* and *iPLA$_2\beta^{+/-}$* on C57BL/6J background) obtained from Dr. John Turk (Washington University School of Medicine, St. Louis, MO) were used to generate wild-type (WT) and iPLA$_2$β-deficient mice at the University of Alabama at Birmingham (UAB), as described [34-36]. PCR validation of genotype was performed using mRNA forward/reverse primers: ccaaacgactttggggagact/ctggatgccgaccatctcg (expected product size, 972 bp). Animal experiments were performed according to approved Institution Animal Care and Use Committee [IACUC] guidelines at UAB.

2.2. Materials.

Reagents used in our studies were obtained from the following sources (catalog numbers): Coomassie reagents, SDS-PAGE reagents, kaleidoscope pre-stained molecular mass standards (161-0324), and Triton X-100 (161-0407) from BioRad, Hercules, CA; *S*-BEL (iPLA$_2$β inhibitor, 10006801), *R*-BEL (iPLA$_2\gamma$ inhibitor, 10006800), CAY10502 (cPLA$_2\alpha$ inhibitor, 10008657), PGE$_2$ (14010), and PGE$_2$ EIA Kit (514010) from Cayman Chemicals, Ann Arbor, MI); paraformaldehyde from Electron Microscopy Sciences, Ft. Washington, PA; acetyl histone H3 antibody (06-911), normal mouse IgG (12-371), protein A beads (16-125) from EMD Millipore, Billerica, MA; Immobilon-P PVDF membrane (IPVH00010) from Millipore Corp., Bedford, MA; Runx2 antibody (D130-3) from MBL International, Wobrurn, MA); arachidonic acid (ICN 19462510) from MP Bio, Solon, OH; GAPDH (FL-335), iPLA$_2$β (sc-14463), tubulin (sc-166729), and 2° (sc-2004, sc-2418, sc-2302) antibodies from Santa Cruz Biotechnology Inc., Santa Cruz, CA; dispase (D4693), protease inhibitor cocktail (P8340), common reagents from Sigma Chemical Co., St. Louis, MO; and alpha-MEM media (12561049), collagenase 2 (17101-015), enhanced chemiluminescence reagent (34095), fetal bovine serum premium (FBS, S11150), and common cell culture reagents from ThermoFisher, Waltham, MA; The EP$_4$ receptor agonist ONO-AE1-329 and EP$_4$ receptor antagonist ONO-AE3-208 were kind gifts from ONO Pharmaceuticals, Osaka, Japan.

2.3. Mineralization Analyses.

(A) Bright field microscopy was performed with an Olympus IX81 microscope; (B) von Kossa staining was performed on fixed cells with a 5% silver nitrate solution [37], rinsed well, and exposed to UV light; and (C) alizarin red staining was performed on fixed cells with a 2% alizarin red solution [38], rinsed well, and scanned for imaging, and quantified using Image J software (National Institutes of Health).

2.4. Primary BMSC Isolation and Analyses.

6-week-old female WT and iPLA$_2$β-deficient mice (KO) were euthanized and femurs surgically isolated. The femurs were transferred to a sterile bio-cabinet before being flushed with alpha-MEM culture media (Con) containing 10% FBS and 1% pen/strep. The media was then centrifuged and cells resuspended in fresh culture media. Plated cells were grown to confluence in the Con media or Ost media (Con media supplemented with 100 μg/ml

ascorbic acid and 10 mM β-glycerol phosphate). In some experiments, cells were treated with the iPLA$_2$β-selective inhibitor *S*-BEL. (10 μM, 30 min treatment at each media change), EP$_4$ receptor agonist (10 μM ONO-AE1-329), or EP$_4$ receptor antagonist (10 μM ONO-AE3-208) and cultured for up to 28 days. The media without and with drugs was replaced every 2 days. Osteogenesis was assessed under bright field microscopy, von Kossa staining, or alizarin red staining.

2.5. Primary Calvaria Isolation and Analyses.

4-day-old female WT and iPLA$_2$β-deficient mice were euthanized and calvaria surgically isolated. The calvaria were transferred to a sterile bio-cabinet before being minced and digested. Digestion media consisted of dispase and collagenase, each at 6 mg/ml. Cells were plated and grown to confluence prior to exposure to Con or Ost media for message analyses by RT-qPCR and osteogenesis assessment using alkaline phosphatase and alizarin red staining. In some experiments the cells were treated with vehicle (DMSO), AA (10 μM), or PGE$_2$ (10 μM) applied at time of differentiation. The media without and with lipids was replaced every 2 days.

2.6. PGE$_2$ Production During Osteogenesis.

MC3T3-E1 cells were cultured and maintained, as described [39]. At 70% confluence, the cells were treated with control or Ost media for 48 h in the absence or presence of *S*-BEL (10 μM), *R*-BEL (10 μM), or CAY10502 (50 nM). The media were collected and PGE$_2$ content was determined using an EIA kit, according to manufacturer's instructions. The cell pellets were processed for protein determination and the data are expressed as pg PGE$_2$/mg protein.

2.7. iPLA$_2$β Induction During Oesteogenesis.

MC3T3-E1 cells were treated with Ost media in the absence or presence of *S*-BEL (10 μM) or PGE$_2$ (10 μM). At 48 h, the cells were harvested, aliquoted, and analyzed by SDS-PAGE. Resolved proteins were transferred from a 10% gel onto Immobilon-PVDF membranes for immunoblotting analyses. Immunoreactive bands were visualized by ECL, as described [40].

2.8. RNA Isolation and RT-qPCR.

Total RNA was isolated, as described [20], and 1 μg of total RNA was reverse-transcribed and analyzed by RT-qPCR using primers sets, based on known mouse sequences (Table 1). The RT-qPCR assays evaluating changes in mRNA levels were performed using validated Taqman primer sets specific for known mouse sequences. Reactions for each sample were performed in triplicate using a PCR protocol (95 °C activation for 10 min followed by 40 cycles of 95 °C for 15 s and 60 °C for 1 min) in an ABI StepOnePlus Detection System (Applied Biosystems, Foster City, CA. *Hprt* was used as the housekeeping control. The Ct values generated by StepOnePlus software (Applied Biosystems) were used to calculate $2^{-\Delta\Delta CT}$ and determine fold change relative to wild type or control conditions.

2.9. Chromatin immunoprecipitation (ChIP) Analyses.

The ChIPs were performed, as described [41]. Cells were grown as described above and nuclei from cross-linked cells were resuspended in Tris/EDTA. The soluble chromatin was adjusted in RIPA buffer and pre-cleared with salmon sperm blocked protein A beads. Immunoprecipitation was performed with 5 μg of antibodies directed against Runx2, Ac-H3, or IgG, as described [42]. Immune complexes were absorbed with protein A beads blocked with salmon sperm DNA. After pre-clearing and before immunoprecipitation, equal amounts of sonicated DNA (10% volume of each sample) were reserved for qPCR (input) analysis. *Pla2g6* and *Runx2* promoters were probed with specific primers against the immunoprecipitated DNA by qPCR using primers sets based on known mouse sequences (Table 2). Several primer sets per each promoter were designed and evaluated, and those that produced a single band with a sufficient melting temperature (≥ 60 °C) were used for the studies described within the manuscript. The qPCR assays evaluating protein-chromatin interactions by ChIP were analyzed using SYBRGreen. Reactions for each sample were performed in triplicate using an ABI StepOnePlus Detection System and a PCR protocol comprising an initial 10 min incubation at 95 °C followed by 40 cycles of 15s at 95 °C and 1 min at 60-65 °C. The raw data were analyzed using StepOnePlus software and ΔΔCt values for each gene in each sample were determined. These studies were repeated three times.

2.10. Drug Concentrations used in this Study.

The chosen concentrations of *S*-BEL. *R*-BEL, and CAY10502 were based on our earlier studies [43,44], and of EP4 ligands and AA on studies in other systems [45-47]. In regards to PGE_2, earlier reports used up to 1 μM [48,49] and in this study 10 μM PGE_2 was used to readily identify outcomes.

2.11. Statistical Analyses.

Data are presented as means ± standard errors of the means [SEMs]. Statistical significance between two groups was determined using the Student's t-test, values of $p < 0.05$ were considered significant. Statistical significances between more than two groups were determined using ANOVA followed by Tukey's post-hoc test. Values of $q\alpha < 0.05$ were considered significant.

3. RESULTS

3.1. Recapitulation of iPLA$_2$β-deficient osteogenesis phenotype in WT BMSCs.

Here, we assessed whether iDLs contribute to bone formation. After confirming the genotype of WT and iPLA$_2$β-deficient (KO) mice, as described [20], BMSCs were prepared from WT and KO mice and PCR analyses used to assess iPLA$_2$β expression. Such analyses yielded an expected product size of 972 bp in WT but not in the KO (Fig. 1A), confirming iPLA$_2$β-deficiency in the KO group. Over 28-days, WT BMSCs exhibited significant mineralization upon exposure to osteogenic media (Ost), as viewed under bright field microscopy (Fig. 1B). In contrast, there was no visual evidence of mineralization in the KO group. To determine whether this defect in osteogenesis was associated with an iPLA$_2$β-deficiency, BMSCs from WT were cultured in the absence or presence of *S*-BEL,

a selective inhibitor of iPLA$_2$β [50], and bone nodule formation was assessed by von Kossa staining. In the absence of *S*-BEL, there was nodule formation in the WT group (Fig. 1C, **top left panel)**. However, with the addition of *S*-BEL, nodule formation was noticeably diminished in the WT group and resembled the low mineralization phenotype of the KO group (in the absence or presence of *S*-BEL, Fig. 1C, **bottom panels**). These findings were taken as evidence for iPLA$_2$β participation in bone formation, with potential involvement of iDLs.

3.2. Rescue of iPLA$_2$β-deficient bone mineralization phenotype by PGE$_2$.

In view of the evidence supporting a role for PGE$_2$ in bone formation and our reports that iPLA$_2$β activation leads to hydrolysis of AA and generation of PGE$_2$ [51,52], we examined the link between PGE$_2$ and bone mineralization. BMSCs isolated from WT and KO were cultured, as above, in Ost media in the absence or presence of *S*-BEL. After 4 days, PGE$_2$ concentration in the media was determined by EIA. In comparison with pre-osteogenic induction, PGE$_2$ levels in the WT group rose nearly 3-fold during osteogenic induction and such increases were inhibited by *S*-BEL. In contrast, increases in PGE$_2$ accumulations were not evident in the KO and were not significantly affected by *S*-BEL treatment (Fig. 2A). In view of these findings, we assessed the impact of PGE$_2$ on mineralization in the iPLA$_2$β-deficient group. Supplementation of the Ost media with PGE$_2$ (Fig. 2B) promoted mineralization, as viewed under bright field microscopy, in comparison with the lack of mineralization in the absence of PGE$_2$ addition. Consistent with this, alizarin red staining, a reflection of calcium deposition, in the KO was reduced, relative to WT, and is increased upon supplementation of the media with PGE$_2$ (Fig. 2C&2E). Quantitation of alizarin red staining revealed a progressive increase in mineralization in the KO over a 28-day period with PGE$_2$ supplementation, that was mimicked by addition of ONO-AE1-329, an EP$_4$ receptor agonist. Moreover, the staining was significantly reduced by co-incubation with ONO-AE3-208, an EP$_4$ receptor antagonist (Fig. 2D). In parallel experiments, we find that under osteogenic conditions alizarin staining increased similarly in WT BMSCs without or with PGE$_2$. However, EP$_4$ receptor antagonism reduced the staining in the WT BMSCs to a level evident in vehicle-treated KO BMSCs under osteogenic conditions (Fig. 2E). These findings suggest a role for PGE$_2$ in facilitating osteogenesis through EP$_4$ receptor signaling.

3.3. iDLs promote expression of osteogenic factors.

We next utilized primary calvarial osteoblasts to gain insight into the osteogenic pathway impacted by iDLs by assessing selected osteogenic factors: BMP2, a TGFβ superfamily member that is important in skeletogenesis and essential for fracture repair, is induced in differentiating osteoblasts and is a hallmark of osteogenesis [53], alkaline phosphatase generates inorganic phosphate that is a requisite for mineralization [53], and Runt-related transcription factor 2 (Runx2) is a master osteogenic transcriptional factor [54]. For these analyses, calvarial osteoblasts from WT and KO mice were prepared and cultured in the absence or presence of *S*-BEL, AA, or PGE$_2$.

As in the BMSCs, calvarial *iPLA$_2$β* mRNA was evident in WT, but nearly undetectable in KO, as determined by RT-qPCR analyses (Fig. 3A). All three osteogenic factors were reduced in the KO group (Figs. 3B-D, ***left panels***), relative to the WT group,

and such decreases were recapitulated in the WT upon treatment with *S*-BEL. However, supplementation of media provided to KO with AA or PGE_2 promoted significant recoveries in all three osteogenic factors (Figs. 3B-D, **right panels**), relative to un-supplemented media. These findings are consistent with a role for iDLs in modulating bone formation.

3.4. Time course of iPLA$_2$β and Runx2 induction in calvarial osteoblasts.

To further address the impact of iDLs on promoting bone mineralization, we focused on Runx2, the master regulator of osteogenesis. Initial examination of temporal induction of *iPLA$_2$β* and *Runx2* revealed a significant rise in both in the WT by 24 h, which was followed by a decline by 36 h (Figs. 4A&B), this effect persisted up to 72 h (data not shown). In the KO group, *iPLA$_2$β* was not detectable or induced and *Runx2* remained unchanged and similar to basal expression over 36 h.

Consistent with these findings, both alkaline phosphatase, reflecting induction of osteogenesis (Fig. 5A, **left panels**), and alizarin red staining, reflecting successful osteogenesis (Fig. 5B, **left panels**), were reduced in the KO, relative to WT, group. Supplementation of media with AA (**middle panels**)> or PGE_2 (**right panels**) resulted in modest increases in alkaline phosphatase in both groups. While alizarin red staining was also only modestly increased in the WT with the supplementations, staining in the KO in the presence of AA or PGE_2 was greater, relative to the vehicle-treated group. Because of recognized limitations in correlating alkaline phosphatase staining with mineralization, alizarin staining was quantified. Such analyses revealed significant increases in mineralization in the KO group, relative to un-supplemented KO group (Fig. 5C), with PGE_2 promoting a near complete recovery. Collectively, these findings strengthen the possibility that PGE_2 derived through iPLA$_2$β-mediated hydrolysis of AA is a key contributor to bone formation.

3.5. Transcriptional regulation of Runx2 and iPLA$_2$β.

To further assess a potential link between iPLA$_2$β and Runx2 during osteoblast differentiation, we performed ChIP assays utilizing primers designed to examine *Runx2* promoters. As expected, analysis of the *Runx2* promoter, known to bind Runx2 protein, revealed association of Runx2 at the *Runx2* promoter (Fig. 6A). These observations correlated with increased detection of Ac-H3, which correlates with transcriptional activation at the *Runx2* gene. IgG control failed to significantly immunoprecipitate *Runx2* promoter.

In silico analyses identified a region of interest for the *Pla2g6* promoter and determined a putative binding site for Runx2 located within 2 kb upstream of the *Pla2g6* transcriptional start site (Fig. 6C). This raised the possibility that Runx2 may drive *Pla2g6* expression. Although Runx2 immunoprecipitation exhibited low binding at the *Pla2g6* promoter that was also not influenced by osteogenic differentiation, there was increased detection of Ac-H3 at the iPLA$_2$β promoter (Fig. 6B), reflecting transcriptional activation at the iPLA$_2$β gene independently of Runx2. These observations correlated with increased detection of Ac-H3, reflecting transcriptional activation at the *Pla2g6* gene. IgG control failed

to significantly immunoprecipitate *iPLA$_2$β* promoter. These data suggest that the *Runx2* promoter is induced under osteogenic conditions but Runx2, itself, does not induce *Pla2g6*.

3.6. Feedback regulation between PGE_2 and $iPLA_2\beta$.

Given the importance of PGE_2 in bone remodeling, we sought to determine the predominant PLA_2 activation that leads to PGE_2 generation during osteogenesis. As these analyses required a greater abundance of cells, the osteoblast precursor cell line, MC3T3-E1, was utilized for analyses. The cells were cultured in Ost media for two days with vehicle (DMSO) only or inhibitors of $iPLA_2\beta$ (*S*-BEL), $iPLA_2\gamma$ (*R*-BEL), or $cPLA_2\alpha$ (CAY10502) (Fig. 7A). As expected, PGE_2 production markedly increased under osteogenic conditions. Such an induction was significantly reduced by *S*-BEL, but not with *R*-BEL or CAY10502. These findings suggest that PGE_2 generated during osteogenesis is mainly derived through $iPLA_2\beta$ activation.

When $iPLA_2\beta$ protein expression during osteogenesis was examined, we found that while it was also induced, it was not significant, relative to Con. This is similar to findings in other systems, where stimuli-induced early increases in $iPLA_2\beta$ protein were noted to taper off well before outcome analyses [55-57]. However, unexpectedly, *S*-BEL also reduced $iPLA_2\beta$ and this was rescued by PGE_2 (Figs. 7B & C). These findings suggest, for the first time, regulation of $iPLA_2\beta$ by $iPLA_2\beta$-derived PGE_2 in osteogenesis.

DISCUSSION

Adult bone is under a constant state of remodeling and the resulting mass and strength of bone are a consequence of balance between bone formation and bone resorption. While certain canonical pathways that influence the bone architecture have been described [2,3,7,8], the potential contribution of lipid signaling is not well understood.

Arachidonic acid (AA), derived via activation of PLA_2s and its cyclooxygenase metabolite, PGE_2, are recognized to induce *Runx2/cbfa1* and *osterix* [58] and have a positive impact on bone formation [22-25]. To date, however, it is not known which PLA_2 provides the lipid signals that are requisite for optimal bone phenotype. In contrast to $cPLA_2\alpha$ or $sPLA_2$s, which are associated with bone resorption [13-19], the $iPLA_2\beta$ appears to participate in bone formation [20].

In the present study, we sought to determine the underlying molecular mechanisms by which lipid signaling derived through $iPLA_2\beta$ activation promotes bone formation. Utilizing multiple models (BMSCs and calvarial osteoblasts from WT and $iPLA_2\beta$-deficient mice and the MC3T3-E1 osteoblast cell line) with analyses (mineralization, mRNA, protein, and ChIP), we find that (a) $iPLA_2\beta$-deficiency leads to significant reductions in osteogenesis and that this phenotype is recapitulated in WT preparations with $iPLA_2\beta$ inhibition; (b) the low bone phenotype is associated with reduced production of PGE_2 and that the osteogenic capacity of $iPLA_2\beta$-deficient preparations is restored by supplementation of the media with PGE_2; (c) expression of *Bmp2, Alpl,* and *Runx2* is reduced with $iPLA_2\beta$-deficiency, recapitulated in WT preparations by the $iPLA_2\beta$ inhibitor, and rescued in $iPLA_2\beta$-deficient preparations with additions of PGE_2; (d) induction of osteogenesis promotes increases in

Runx2 and *iPLA$_2$β* mRNA; and (e) during osteogenesis, iPLA$_2$β protein expression is reduced by iPLA$_2$β inhibitor and rescued with addition of PGE$_2$.

Collectively, our findings reveal the importance of iDLs in bone formation, where activation of iPLA$_2$β in osteoblasts leads to hydrolysis of AA, which is then metabolized to PGE$_2$ by COX-2. The PGE$_2$ acting via EP$_4$ receptor triggers signaling pathways leading to induction of osteogenesis factors. This proposed mechanism is supported by the findings that (a) the decreases in mineralization and associated osteogenic factors expression are evident in an iPLA$_2$β-deficient model, (b) these outcomes are rescued by addition of AA or PGE$_2$, (c) osteogenesis in the KO is similarly rescued with PGE$_2$ or EP$_4$ receptor agonism, (d) EP$_4$ receptor antagonism reduces osteogenesis in WT to KO levels, and (e) production of PGE$_2$ is mitigated by inhibition of iPLA$_2$β, but not of iPLA$_2$γ or cPLA$_2$α. Given that iPLA$_2$s and sPLA$_2$s exhibit non-specific hydrolysis of *sn*-2 substituents and cPLA$_2$α is selective for arachidonic acid [59-62], our observations suggest that the predominant pool of PGE$_2$ that contributes to bone formation is derived through iPLA$_2$β-catalyzed hydrolysis of AA from membrane glycerophospholipids.

The observation that the impact of PGE$_2$ supplementation was in general more profound than with AA is likely due to multiple factors: AA can be metabolized by multiple enzymes [63], incorporated into phospholipids, or be a substrate for elongases [64]. Thus, not all added AA is likely to be converted to PGE$_2$. It has been reported that the predominant receptor activated by PGE$_2$ in calvarial osteoblastic cell cultures is the EP$_4$ receptor [48]. While the mechanism by which PGE$_2$ induces Runx2 was not examined here, a recent report suggests that PGE$_2$ signaling via $_{EP4}$ receptor can promote gene transcription [65]. Taken together with the observations of EP$_4$ receptor localization also in the nuclear envelope [66] and the presence of COX and PGE$_2$ in the nuclear membrane [67], we posit that iPLA$_2$β-derived PGE$_2$, through EP$_4$ receptor signaling, leads to Runx2 induction.

Among our observations, an unexpected finding was that selective inhibition of iPLA$_2$β decreased iPLA$_2$β protein expression. Moreover, addition of PGE$_2$ rescued this outcome. These findings reveal, a previously unrecognized, feedback regulation of iPLA$_2$β by lipid products derived from iPLA$_2$β activation. In a recent study, we reported that expression of *Ptgs2,* which encodes COX-2, is reduced in iPLA$_2$β-KO macrophages [68]. We speculate that inhibition of iPLA$_2$β, in addition to providing less AA as a substrate for eicosanoid generation via COX-2, also mitigates COX-2 expression in osteoblast cells with the consequent decrease in PGE$_2$ production leading to mitigation of iPLA$_2$β expression. Further studies are needed to delineate specific feedback mechanisms by which iDLs can impact iPLA$_2$β expression.

In summary (Fig. 8), our findings provide a scheme for iPLA$_2$β participation in bone formation. Our results indicate that iPLA$_2$β activation plays important roles in the dynamic process of bone formation and maintenance. Under osteogenesis stimuli, iPLA$_2$β induction leads to accumulation of AA and generation of PGE$_2$, leading to induction of Runx2 and iPLA$_2$β. These observations suggest that modulation of the iPLA$_2$β-Runx2 axis could be an avenue to improve bone health in diseased states associated with compromised bone formation.

ACKNOWLEDGEMENTS

We thank the support of the Department of CDIB, UAB Center for Metabolic Bone Disorders, UAB Comprehensive Diabetes Center and Diabetes Research Center, and Dr. Amjad Javed for offering advice on the RT-qPCR analyses.

FUNDING SOURCES

Work at UAB was supported by funds from The Department of CDIB, and grants from the UAB Center for Metabolic Bone Disease (NIH P30AR046031), NIH/NIDDK (DK-69455 and DK-110292 to SR; P30DK079626 to UAB DRC), Department of Veterans Affairs (VA Merit Review I01 BX001370 to GAC), and NIH/NCI (R01CA138517 to SEN).

Abbreviations:

18S	18S ribosomal RNA
Ac-H3	acetylated histone H3
AA	arachidonic acid
Alpl	alkaline phosphatase
BMSCs	bone marrow stromal cells
Bmp2	bone morphogenetic protein 2
ChIP	chromatin immunoprecipitation
COX	cyclooxygenase
cPLA$_2$α	cytosolic phospholipase A$_2$α
DMSO	dimethyl sulfoxide
EIA	enzyme immunoassay
GAPDH	glyceraldehyde 3-phosphate dehydrogenase
Hprt	hypoxanthine phosphoribosyltransferase
IgG	immunoglobulin G
iDLs	iPLA$_2$β-derived lipids
iPLA$_2$β	group VIA phospholipase A$_2$ beta
iPLA$_2$γ	group VIB phospholipase A$_2$gamma
KO	knockout
12-LO	12-lipoxygenase
PCR	polymerase chain reaction
PGE$_2$	prostaglandin E$_2$
PLA$_2$	phospholipase A$_2$

***R*-BEL**	*R*-enantiomer of bromoenol lactone
RT-qPCR	real time quantitative PCR
Runx2	Runt-related transcription factor 2
***S*-BEL**	*S*-enantiomer of bromoenol lactone
WT	wild type

REFERENCES

1. Albrand G;Munoz F;Sornay-Rendu E;Duboeuf F;Delmas PD Independent predictors of all osteoporosis-related fractures in healthy postmenopausal women: the OFELY study. Bone. 32 (2003) 78–85. 10.1016/s8756-3282(02)00919-5. [PubMed: 12584039]
2. Burr DB Bone material properties and mineral matrix contributions to fracture risk or age in women and men. J Musculoskelet Neuronal Interact. 2 (2002) 201–204. [PubMed: 15758433]
3. Espallargues M;Sampietro-Colom L;Estrada MD;Sola M;Del Rio L;Setoain J;Granados A Identifying bone-mass-related risk factors for fracture to guide bone densitometry measurements: a systematic review of the literature. Osteoporos Int. 12 (2001) 811–822. 10.1007/s001980170031. [PubMed: 11716183]
4. Moerman EJ;Teng K;Lipschitz DA;Lecka-Czernik B Aging activates adipogenic and suppresses osteogenic programs in mesenchymal marrow stroma/stem cells: the role of PPAR-gamma2 transcription factor and TGF-beta/BMP signaling pathways. Aging Cell. 3 (2004) 379–389. 10.1111/j.1474-9728.2004.00127.x. [PubMed: 15569355]
5. Perrien DS;Akel NS;Dupont-Versteegden EE;Skinner RA;Siegel ER;Suva LJ;Gaddy D Aging alters the skeletal response to disuse in the rat. Am J Physiol Regul Integr Comp Physiol. 292 (2007) R988–996. 10.1152/ajpregu.00302.2006. [PubMed: 17068163]
6. Rittweger J;Gunga HC;Felsenberg D;Kirsch KA Muscle and bone-aging and space. J Gravit Physiol. 6 (1999) P133–136. [PubMed: 11542992]
7. Suva LJ;Gaddy D;Perrien DS;Thomas RL;Findlay DM Regulation of bone mass by mechanical loading: microarchitecture and genetics. Curr Osteoporos Rep. 3 (2005) 46–51. 10.1007/s11914-005-0003-0. [PubMed: 16036101]
8. Chesnut CH 3rd. Osteoporosis, an underdiagnosed disease. JAMA. 286 (2001) 2865–2866. 10.1001/jama.286.22.2865. [PubMed: 11735763]
9. Das UN Is There a role for bioactive lipids in the pathobiology of diabetes mellitus? Front Endocrinol (Lausanne). 8 (2017) 182. 10.3389/fendo.2017.00182. [PubMed: 28824543]
10. Gilroy DW;Newson J;Sawmynaden P;Willoughby DA;Croxtall JD A novel role for phospholipase A_2 isoforms in the checkpoint control of acute inflammation. FASEB J. 18 (2004) 489–498. 10.1096/fj.03-0837com. [PubMed: 15003994]
11. Murakami M;Kambe-Ohkura T;Kudo I Functional coupling between phospholipase A_2S and cyclooxygenases in immediate and delayed prostanoid biosynthetic pathways. Adv Exp Med Biol. 507 (2002) 15–19. 10.1007/978-1-4615-0193-0_3. [PubMed: 12664558]
12. Ramanadham S;Song H;Hsu FF;Zhang S;Crankshaw M;Grant GA;Newgard CB;Bao S;Ma Z;Turk J Pancreatic islets and insulinoma cells express a novel isoform of group VIA phospholipase A_2 ($iPLA_2\beta$) that participates in glucose-stimulated insulin secretion and is not produced by alternate splicing of the $iPLA_2$ beta transcript. Biochemistry. 42 (2003) 13929–13940. 10.1021/bi034843p. [PubMed: 14636061]
13. Ellies LG;Heersche JN;Pruzanski W;Vadas P;Aubin JE The role of phospholipase A_2 in interleukin-1 alpha-mediated inhibition of mineralization of the osteoid formed by fetal rat calvaria cells in vitro. J Dent Res. 72 (1993) 18–24. 10.1177/00220345930720010101. [PubMed: 8418103]
14. Gregory LS;Kelly WL;Reid RC;Fairlie DP;Forwood MR Inhibitors of cyclo-oxygenase-2 and secretory phospholipase A_2 preserve bone architecture following ovariectomy in adult rats. Bone. 39 (2006) 134–142. 10.1016/j.bone.2005.12.017. [PubMed: 16473054]

15. Macdonald BR;Gallagher JA;Ahnfelt-Ronne I;Beresford JN;Gowen M;Russell RG Effects of bovine parathyroid hormone and 1,25-dihydroxyvitamin D3 on the production of prostaglandins by cells derived from human bone. FEBS Lett. 169 (1984) 49–52. 10.1016/0014-5793(84)80287-2. [PubMed: 6425082]
16. Meghji S;Sandy JR;Scutt AM;Harvey W;Harris M Stimulation of bone resorption by lipoxygenase metabolites of arachidonic acid. Prostaglandins. 36 (1988) 139–149. 10.1016/0090-6980(88)90301-2. [PubMed: 2847250]
17. Miyahara T;Tonoyama H;Watanabe M;Okajima A;Miyajima S;Sakuma T;Nemoto N;Takayama K Stimulative effect of cadmium on prostaglandin E_2 production in primary mouse osteoblastic cells. Calcif Tissue Int. 68 (2001) 185–191. 10.1007/s002230001216. [PubMed: 11351503]
18. Miyaura C;Inada M;Matsumoto C;Ohshiba T;Uozumi N;Shimizu T;Ito A An essential role of cytosolic phospholipase A_2alpha in prostaglandin E_2-mediated bone resorption associated with inflammation. J Exp Med. 197 (2003) 1303–1310. 10.1084/jem.20030015. [PubMed: 12743173]
19. Traianedes K;Dallas MR;Garrett IR;Mundy GR;Bonewald LF 5-Lipoxygenase metabolites inhibit bone formation *in vitro*. Endocrinology. 139 (1998) 3178–3184. 10.1210/endo.139.7.6115. [PubMed: 9645691]
20. Ramanadham S;Yarasheski KE;Silva MJ;Wohltmann M;Novack DV;Christiansen B;Tu X;Zhang S;Lei X;Turk J Age-related changes in bone morphology are accelerated in group VIA phospholipase A_2 ($iPLA_2\beta$)-null mice. Am J Pathol. 172 (2008) 868–881. 10.2353/ajpath.2008.070756. [PubMed: 18349124]
21. Gijon MA;Leslie CC Phospholipases A_2. Semin Cell Dev Biol. 8 (1997) 297–303. 10.1006/scdb.1997.0151. [PubMed: 10024493]
22. Weiler HA Dietary supplementation of arachidonic acid is associated with higher whole body weight and bone mineral density in growing pigs. Pediatr Res. 47 (2000) 692–697. 10.1203/00006450-200005000-00022. [PubMed: 10813598]
23. Breyer RM;Bagdassarian CK;Myers SA;Breyer MD Prostanoid receptors: subtypes and signaling. Annu Rev Pharmacol Toxicol. 41 (2001) 661–690. 10.1146/annurev.pharmtox.41.1.661. [PubMed: 11264472]
24. Narumiya S;Sugimoto Y;Ushikubi F Prostanoid receptors: structures, properties, and functions. Physiol Rev. 79 (1999) 1193–1226. 10.1152/physrev.1999.79.4.1193. [PubMed: 10508233]
25. Forwood MR Inducible cyclo-oxygenase (COX-2) mediates the induction of bone formation by mechanical loading in vivo. J Bone Miner Res. 11 (1996) 1688–1693. 10.1002/jbmr.5650111112. [PubMed: 8915776]
26. Chen QR;Miyaura C;Higashi S;Murakami M;Kudo I;Saito S;Hiraide T;Shibasaki Y;Suda T Activation of cytosolic phospholipase A_2 by platelet-derived growth factor is essential for cyclooxygenase-2-dependent prostaglandin E_2 synthesis in mouse osteoblasts cultured with interleukin-1. J Biol Chem. 272 (1997) 5952–5958. 10.1074/jbc.272.9.5952. [PubMed: 9038215]
27. Jee WS;Ueno K;Deng YP;Woodbury DM The effects of prostaglandin E_2 in growing rats: increased metaphyseal hard tissue and cortico-endosteal bone formation. Calcif Tissue Int. 37 (1985) 148–157. 10.1007/BF02554834. [PubMed: 3924371]
28. Lucia VD;Fitzpatrick-Wong SC;Weiler HA Dietary arachidonic acid suppresses bone turnover in contrast to low dosage exogenous prostaglandin E_2 that elevates bone formation in the piglet. Prostaglandins Leukot Essent Fatty Acids. 68 (2003) 407–413. 10.1016/s0952-3278(03)00065-6. [PubMed: 12798661]
29. Tai H;Miyaura C;Pilbeam CC;Tamura T;Ohsugi Y;Koishihara Y;Kubodera N;Kawaguchi H;Raisz LG;Suda T Transcriptional induction of cyclooxygenase-2 in osteoblasts is involved in interleukin-6-induced osteoclast formation. Endocrinology. 138 (1997) 2372–2379. 10.1210/endo.138.6.5192. [PubMed: 9165025]
30. Machwate M;Harada S;Leu CT;Seedor G;Labelle M;Gallant M;Hutchins S;Lachance N;Sawyer N;Slipetz D;Metters KM;Rodan SB;Young R;Rodan GA Prostaglandin receptor EP_4 mediates the bone anabolic effects of PGE_2. Mol Pharmacol. 60 (2001) 36–41. 10.1124/mol.60.1.36. [PubMed: 11408598]

31. Mori S;Jee WS;Li XJ;Chan S;Kimmel DB Effects of prostaglandin E_2 on production of new cancellous bone in the axial skeleton of ovariectomized rats. Bone. 11 (1990) 103–113. 10.1016/8756-3282(90)90057-6. [PubMed: 2192750]
32. Sakuma Y;Tanaka K;Suda M;Komatsu Y;Yasoda A;Miura M;Ozasa A;Narumiya S;Sugimoto Y;Ichikawa A;Ushikubi F;Nakao K Impaired bone resorption by lipopolysaccharide *in vivo* in mice deficient in the prostaglandin E receptor EP_4 subtype. Infect Immun. 68 (2000) 6819–6825. 10.1128/iai.68.12.6819-6825.2000. [PubMed: 11083800]
33. Yoshida K;Oida H;Kobayashi T;Maruyama T;Tanaka M;Katayama T;Yamaguchi K;Segi E;Tsuboyama T;Matsushita M;Ito K;Ito Y;Sugimoto Y;Ushikubi F;Ohuchida S;Kondo K;Nakamura T;Narumiya S Stimulation of bone formation and prevention of bone loss by prostaglandin E EP_4 receptor activation. Proc Natl Acad Sci U S A. 99 (2002) 4580–4585. 10.1073/pnas.062053399. [PubMed: 11917107]
34. Bao S;Jacobson DA;Wohltmann M;Bohrer A;Jin W;Philipson LH;Turk J Glucose homeostasis, insulin secretion, and islet phospholipids in mice that overexpress $iPLA_2\beta$ in pancreatic beta-cells and in $iPLA_2\beta$-null mice. Am J Physiol Endocrinol Metab. 294 (2008) E217–229. 10.1152/ajpendo.00474.2007. [PubMed: 17895289]
35. Bao S;Miller DJ;Ma Z;Wohltmann M;Eng G;Ramanadham S;Moley K;Turk J Male mice that do not express group VIA phospholipase A_2 produce spermatozoa with impaired motility and have greatly reduced fertility. J Biol Chem. 279 (2004) 38194–38200. 10.1074/jbc.M406489200. [PubMed: 15252026]
36. Lei X;Bone RN;Ali T;Wohltmann M;Gai Y;Goodwin KJ;Bohrer AE;Turk J;Ramanadham S Genetic modulation of islet beta-cell $iPLA_2\beta$ expression provides evidence for its impact on beta-cell apoptosis and autophagy. Islets. 5 (2013) 29–44. 10.4161/isl.23758. [PubMed: 23411472]
37. Tu X;Joeng KS;Nakayama KI;Nakayama K;Rajagopal J;Carroll TJ;Mcmahon AP;Long F Noncanonical Wnt signaling through G protein-linked PKCdelta activation promotes bone formation. Dev Cell. 12 (2007) 113–127. 10.1016/j.devcel.2006.11.003. [PubMed: 17199045]
38. Silva MJ;Brodt MD Mechanical stimulation of bone formation is normal in the SAMP6 mouse. Calcif Tissue Int. 82 (2008) 489–497. 10.1007/s00223-008-9142-5. [PubMed: 18509697]
39. Clines GA;Mohammad KS;Grunda JM;Clines KL;Niewolna M;Mckenna CR;Mckibbin CR;Yanagisawa M;Suva LJ;Chirgwin JM;Guise TA Regulation of postnatal trabecular bone formation by the osteoblast endothelin A receptor. J Bone Miner Res. 26 (2011) 2523–2536. 10.1002/jbmr.450. [PubMed: 21698666]
40. Adhami MD;Rashid H;Chen H;Clarke JC;Yang Y;Javed, A. Loss of Runx2 in committed osteoblasts impairs postnatal skeletogenesis. J Bone Miner Res. 30 (2015) 71–82. 10.1002/jbmr.2321. [PubMed: 25079226]
41. Nozell S;Laver T;Patel K;Benveniste EN Mechanism of IFN-beta-mediated inhibition of IL-8 gene expression in astroglioma cells. J Immunol. 177 (2006) 822–830. 10.4049/jimmunol.177.2.822. [PubMed: 16818736]
42. Mcfarland BC;Hong SW;Rajbhandari R;Twitty GB Jr.;Gray GK;Yu H;Benveniste EN;Nozell SE NF-kappaB-induced IL-6 ensures STAT3 activation and tumor aggressiveness in glioblastoma. PLoS One. 8 (2013) e78728. 10.1371/journal.pone.0078728. [PubMed: 24244348]
43. Ali T;Kokotos G;Magrioti V;Bone RN;Mobley JA;Hancock W;Ramanadham S Characterization of FKGK18 as inhibitor of group VIA Ca^{2+}-independent phospholipase A_2 ($iPLA_2\beta$): candidate drug for preventing beta-cell apoptosis and diabetes. PLoS One. 8 (2013) e71748. 10.1371/journal.pone.0071748. [PubMed: 23977134]
44. Nelson AJ;Stephenson DJ;Cardona CL;Lei X;Almutairi A;White TD;Tusing YG;Park MA;Barbour SE;Chalfant CE;Ramanadham S Macrophage polarization is linked to Ca^{2+}-independent phospholipase A_2beta-derived lipids and cross-cell signaling in mice. J Lipid Res. 61 (2020) 143–158. 10.1194/jlr.RA119000281. [PubMed: 31818877]
45. Nakatsuji M;Minami M;Seno H;Yasui M;Komekado H;Higuchi S;Fujikawa R;Nakanishi Y;Fukuda A;Kawada K;Sakai Y;Kita T;Libby P;Ikeuchi H;Yokode M;Chiba T EP_4 Receptor-associated protein in macrophages ameliorates colitis and colitis-associated tumorigenesis. PLoS Genet. 11 (2015) e1005542. 10.1371/journal.pgen.1005542. [PubMed: 26439841]
46. Safholm J;Dahlen SE;Delin I;Maxey K;Stark K;Cardell LO;Adner M PGE_2 maintains the tone of the guinea pig trachea through a balance between activation of contractile EP_1 receptors and

relaxant EP_2 receptors. Br J Pharmacol. 168 (2013) 794–806. 10.1111/j.1476-5381.2012.02189.x. [PubMed: 22934927]

47. Persaud SJ;Muller D;Belin VD;Kitsou-Mylona I;Asare-Anane H;Papadimitriou A;Burns CJ;Huang GC;Amiel SA;Jones PM The role of arachidonic acid and its metabolites in insulin secretion from human islets of langerhans. Diabetes. 56 (2007) 197–203. 10.2337/db06-0490. [PubMed: 17192482]
48. Alander CB;Raisz LG Effects of selective prostaglandins E_2 receptor agonists on cultured calvarial murine osteoblastic cells. Prostaglandins Other Lipid Mediat. 81 (2006) 178–183. 10.1016/j.prostaglandins.2006.09.005. [PubMed: 17085326]
49. Gao Q;Zhan P;Alander CB;Kream BE;Hao C;Breyer MD;Pilbeam CC;Raisz LG Effects of global or targeted deletion of the EP_4 receptor on the response of osteoblasts to prostaglandin *in vitro* and on bone histomorphometry in aged mice. Bone. 45 (2009) 98–103. 10.1016/j.bone.2009.03.667. [PubMed: 19344793]
50. Jenkins CM;Han X;Mancuso DJ;Gross RW Identification of calcium-independent phospholipase A_2 (iPLA$_2$) beta, and not iPLA$_2$gamma, as the mediator of arginine vasopressin-induced arachidonic acid release in A-10 smooth muscle cells. Enantioselective mechanism-based discrimination of mammalian iPLA$_2$s. J Biol Chem. 277 (2002) 32807–32814. 10.1074/jbc.M202568200. [PubMed: 12089145]
51. Ramanadham S;Gross RW;Han X;Turk J Inhibition of arachidonate release by secretagogue-stimulated pancreatic islets suppresses both insulin secretion and the rise in beta-cell cytosolic calcium ion concentration. Biochemistry. 32 (1993) 337–346. 10.1021/bi00052a042. [PubMed: 8418854]
52. Ramanadham S;Hsu FF;Bohrer A;Ma Z;Turk J Studies of the role of group VI phospholipase A_2 in fatty acid incorporation, phospholipid remodeling, lysophosphatidylcholine generation, and secretagogue-induced arachidonic acid release in pancreatic islets and insulinoma cells. J Biol Chem. 274 (1999) 13915–13927. 10.1074/jbc.274.20.13915. [PubMed: 10318801]
53. Bilezikian JP;Raisz LG;Rodan GA Principles of bone biology. San Diego: Academic Press, 2002.
54. Javed A;Afzal F;Bae JS;Gutierrez S;Zaidi K;Pratap J;Van Wijnen AJ;Stein JL;Stein GS;Lian JB Specific residues of RUNX2 are obligatory for formation of BMP2-induced RUNX2-SMAD complex to promote osteoblast differentiation. Cells Tissues Organs. 189 (2009) 133–137. 10.1159/000151719. [PubMed: 18728344]
55. Lei X;Zhang S;Bohrer A;Bao S;Song H;Ramanadham S The group VIA calcium-independent phospholipase A_2 participates in ER stress-induced INS-1 insulinoma cell apoptosis by promoting ceramide generation via hydrolysis of sphingomyelins by neutral sphingomyelinase. Biochemistry. 46 (2007) 10170–10185. 10.1021/bi700017z. [PubMed: 17685585]
56. Fei X;Zhang S;Bohrer A;Ramanadham S Calcium-independent phospholipase A_2 (iPLA$_2$ beta)-mediated ceramide generation plays a key role in the cross-talk between the endoplasmic reticulum (ER) and mitochondria during ER stress-induced insulin-secreting cell apoptosis. J Biol Chem. 283 (2008) 34819–34832. 10.1074/jbc.M807409200. [PubMed: 18936091]
57. Ramanadham S;Hsu FF;Zhang S;Jin C;Bohrer A;Song H;Bao S;Ma Z;Turk J Apoptosis of insulin-secreting cells induced by endoplasmic reticulum stress is amplified by overexpression of group VIA calcium-independent phospholipase A_2 (iPFA$_2$β) and suppressed by inhibition of iPLA$_2$β. Biochemistry. 43 (2004) 918–930. 10.1021/bi035536m. [PubMed: 14744135]
58. Zhang X;Schwarz EM;Young DA;Puzas JE;Rosier RN;O'keefe RJ Cyclooxygenase-2 regulates mesenchymal cell differentiation into the osteoblast lineage and is critically involved in bone repair. J Clin Invest. 109 (2002) 1405–1415. 10.1172/JCI15681. [PubMed: 12045254]
59. Liu GY;Moon SH;Jenkins CM;Li M;Sims HF;Guan S;Gross RW The phospholipase iPLA$_2$gamma is a major mediator releasing oxidized aliphatic chains from cardiolipin, integrating mitochondrial bioenergetics and signaling. J Biol Chem. 292 (2017) 10672–10684. 10.1074/jbc.M117.783068. [PubMed: 28442572]
60. Mouchlis VD;Chen Y;Mccammon JA;Dennis EA Membrane allostery and unique hydrophobic sites promote enzyme substrate specificity. J Am Chem Soc. 140 (2018) 3285–3291. 10.1021/jacs.7b12045. [PubMed: 29342349]
61. Murakami M;Sato H;Taketomi Y Updating phospholipase A_2 biology. Biomolecules. 10 (2020) 10.3390/biom10101457.

62. Yoda E;Rai K;Ogawa M;Takakura Y;Kuwata H;Suzuki H;Nakatani Y;Murakami M;Hara S Group VIB calcium-independent phospholipase A_2 (iPLA_2gamma) regulates platelet activation, hemostasis and thrombosis in mice. PLoS One. 9 (2014) e109409. 10.1371/journal.pone.0109409. [PubMed: 25313821]

63. Wang B;Wu L;Chen J;Dong L;Chen C;Wen Z;Hu J;Fleming I;Wang DW Metabolism pathways of arachidonic acids: mechanisms and potential therapeutic targets. Signal Transduct Target Ther. 6 (2021) 94. 10.1038/s41392-020-00443-w. [PubMed: 33637672]

64. Ramanadham S;Zhang S;Ma Z;Wohltmann M;Bohrer A;Hsu FF;Turk J Delta6-, Stearoyl CoA-, and Delta5-desaturase enzymes are expressed in beta-cells and are altered by increases in exogenous PUFA concentrations. Biochim Biophys Acta. 1580 (2002) 40–56. 10.1016/s1388-1981(01)00189-5. [PubMed: 11923099]

65. Maeda Y;Sekiguchi F;Yamanaka R;Sugimoto R;Yamasoba D;Tomita S;Nishikawa H;Kawabata A Mechanisms for proteinase-activated receptor 1-triggered prostaglandin E_2 generation in mouse osteoblastic MC3T3-E1 cells. Biol Chem. 396 (2015) 153–162. 10.1515/hsz-2014-0148. [PubMed: 25205726]

66. Bhattacharya M;Peri KG;Almazan G;Ribeiro-Da-Silva A;Shichi H;Durocher Y;Abramovitz M;Hou X;Varma DR;Chemtob S Nuclear localization of prostaglandin E_2 receptors. Proc Natl Acad Sci U S A. 95 (1998) 15792–15797. 10.1073/pnas.95.26.15792. [PubMed: 9861049]

67. Spencer AG;Woods JW;Arakawa T;Singer Ii;Smith WL Subcellular localization of prostaglandin endoperoxide H synthases-1 and −2 by immunoelectron microscopy. J Biol Chem. 273 (1998) 9886–9893. 10.1074/jbc.273.16.9886. [PubMed: 9545330]

68. Ashley JW;Hancock WD;Nelson AJ;Bone RN;Tse HM;Wohltmann M;Turk J;Ramanadham S Polarization of macrophages toward M2 phenotype is favored by reduction in iPLA_2beta (group VIA phospholipase A_2). J Biol Chem. 291 (2016) 23268–23281. 10.1074/jbc.M116.754945. [PubMed: 27650501]

Highlights

- $iPLA_2\beta$-derived PGE_2 is important for optimal bone formation
- $iPLA_2\beta$-derived PGE_2 induces osteogenic factors
- Select inhibitors of $iPLA_2\beta$ and EP4 receptor mitigate induction of osteogenic factors and osteogenesis
- Roles for $iPLA_2\beta$-derived PGE_2 include induction of Runx2 and also $iPLA_2\beta$
- First demonstration of $iPLA_2\beta$ regulation by downstream products of its activation

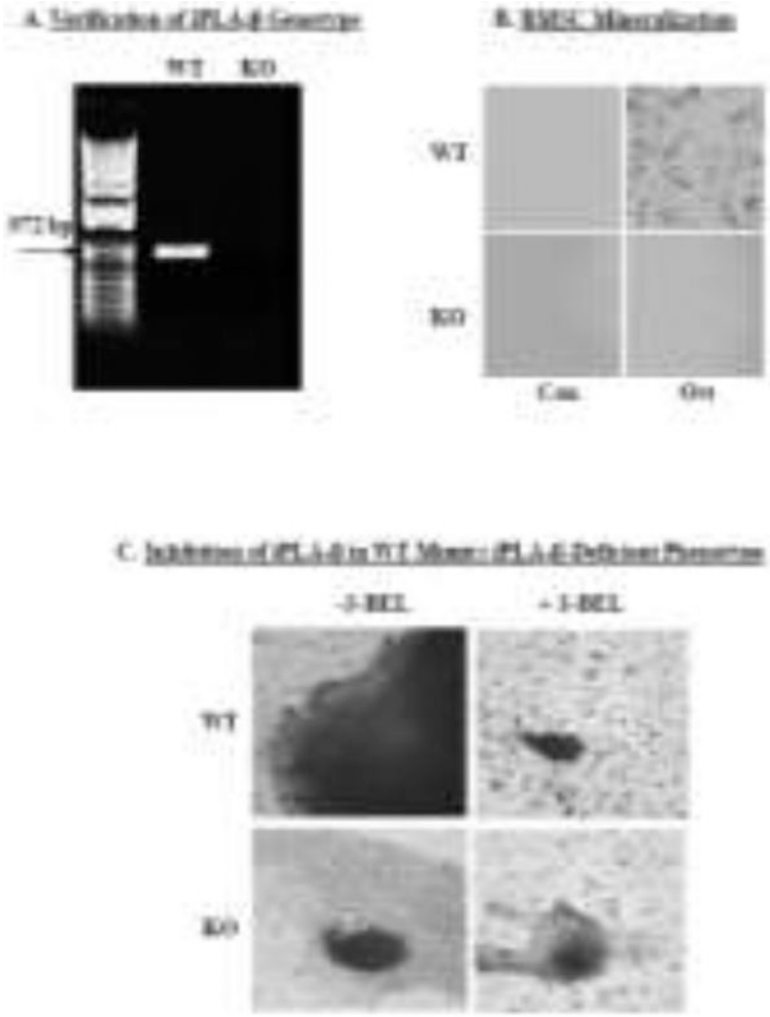

Fig. 1. *In vitro* mineralization of WT and iPLA$_2$β-deficient BMSCs.

Bone marrow stromal cells (BMSCs) from WT and iPLA$_2$β-deficient (KO) mice were harvested for analyses. *A*, Genotyping. Validation of iPLA$_2$β-deficient genotype via PCR. *B*, Mineralization. WT and KO BMSCs were exposed to Con or Ost (100 μg/ml ascorbic acid and 10 mM β-glycerol phosphate) media for 28 days and mineralization was assessed under bright field microscopy (4X magnification). *C*, Bone nodule formation. WT and KO BMSCs were cultured with Ost media for 28 days without and with *S*-BEL (10 μM) and bone nodule formation was assessed by von Kossa staining (20X magnification).

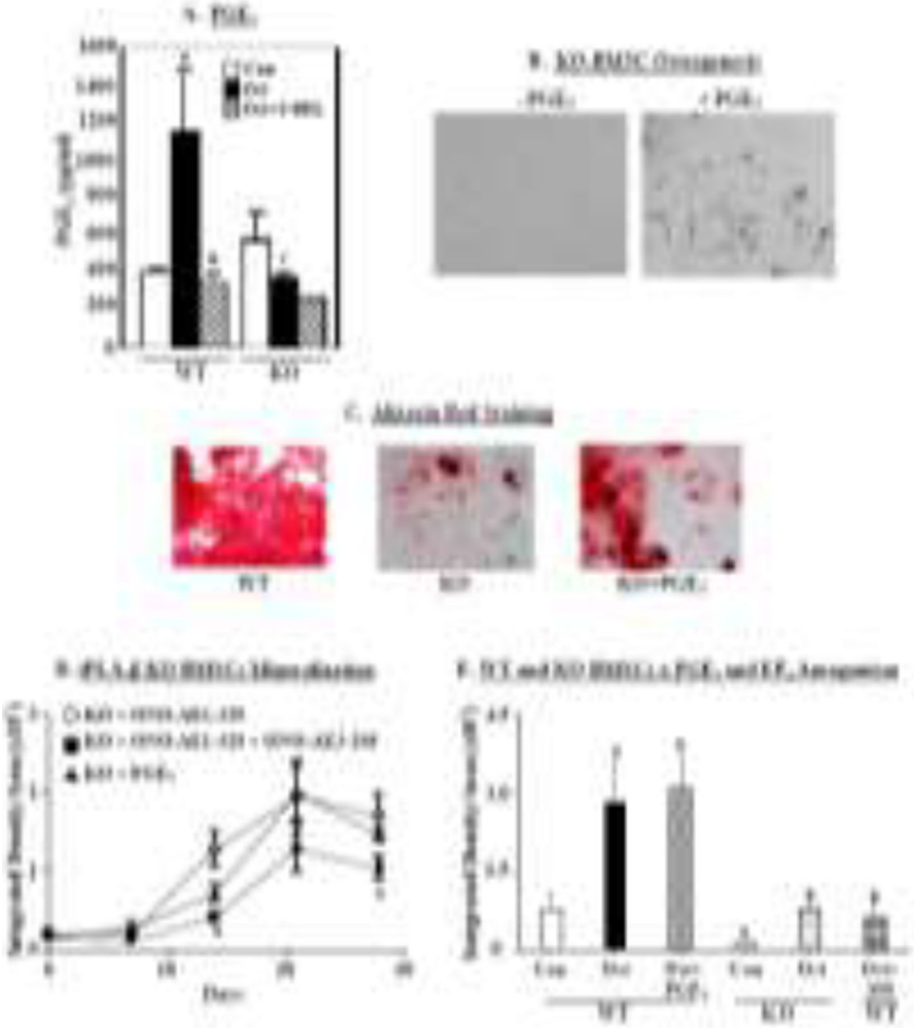

Fig. 2. Rescue of iPLA$_2$β-deficient bone mineralization phenotype with PGE$_2$ supplementation.
A, PGE$_2$production. BMSCs were harvested from WT and KO mice and cultured in Con or Ost media in the absence or presence of *S*-BEL (10 μM). At 4 days, media accumulations in PGE$_2$ were determined by EIA. Data are the means ± SEMs (4-5 independent measurements). ([a]Significantly different from WT Con, $p < 0.01$; [b]significantly different from WT Ost, $p < 0.005$; [c]significantly different from WT Ost, $p < 0.01$.) *B*, Osteogenesis in the absence or presence of PGE$_2$. BMSCs harvested from iPLA$_2$β-deficient mice were cultured in Ost media without or with PGE$_2$ (10 μM) supplementation and visualized under bright field microscopy (4X magnification). *C*, Mineralization in the absence or presence of PGE$_2$. BMSCs harvested from WT and KO mice were cultured in Ost media in the absence or presence of PGE$_2$ (10 μM). Representative images of alizarin staining are shown (4X magnification). *D*, Mineralization quantification. BMSCs harvested from WT and KO mice were cultured in media supplemented with PGE$_2$ (10 μM), ONO-AE1-329 (EP$_4$ receptor agonist, 10 μM), or ONO-AE3-208 (EP$_4$ receptor antagonist, 10 μM) at each media change. Alizarin staining was quantified by ImageJ analysis. Data are the means ± SEMs (3 independent measurements). ([a]EP$_4$ antagonist group significantly different from EP$_4$ agonist group, $p < 0.05$.). *E*, EP$_4$ receptor antagonism in WT recapitulates osteogenesis

in KO. BMSCs from WT and KO mice were cultured in Con or Ost media, furthermore WT were also treated in Ost media in the absence or presence of PGE_2 or ONO-AE3-208, as in *D.* In the absence of these additions, vehicle was included in the culture media. Alizarin staining at 20 days (peak time) was quantified. ([a]Significantly different from WT Con, $p < 0.05$; [b]significantly different from WT Ost, $p < 0.05$.)

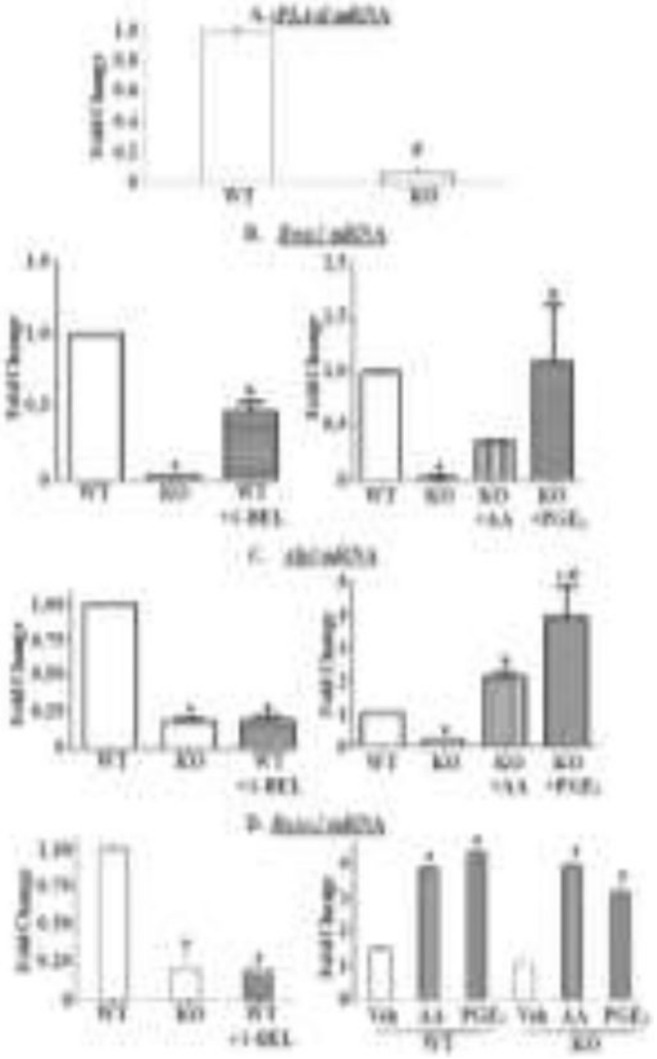

Fig. 3. Impact of iPLA$_2$β-derived lipids on osteogenic factors in calvarial osteoblasts.

Calvarial osteoblasts were prepared from 4-day old female WT and KO mice. *A*, Genotype verification. The cells were processed for *iPLA$_2$β* mRNA analyses by RT-qPCR. *B-D*, Osteogenic factors. The cells were cultured for 7 days in Ost media in the presence of vehicle only or with *S*-BEL (10 μM), AA (10 μM), or PGE_2 (10 μM) at each media change. The cells were then processed for RT-qPCR analyses for *Bmp2* (*B*), *Alpl* (*C*), and *Runx2* (*D*). *Hprt* was used as housekeeping control. Data are the means ± SEMs (3 independent measurements). *D* (*right panel*) represents fold-changes in each genotype relative to own Con (undifferentiated media). All other panels represent fold-changes relative to WT Ost. (*A*, #KO group significantly different from age-matched WT group, $p < 0.05$. *B (left panel)*, [a]significantly different from WT, $p < 0.001$; [b]significantly different from WT and KO (Ost), $p < 0.001$. *B (right panel)*, [a]significantly different from WT, $p < 0.001$; [b]significantly different from KO, $p < 0.05$. *C (left panel)*, [a]significantly different from WT, $p < 0.001$. *C (right panel)*, [a]significantly different from WT, $p < 0.001$; [b]significantly different from KO, $p < 0.05$; [c]significantly different from KO, $p < 0.001$; [d]significantly different from

KO+AA, $p < 0.05$. *D (left panel)*, [a]significantly different from WT, $p < 0.001$; *D (right panel)*, [a]significantly different from corresponding vehicle, $p < 0.05$.)

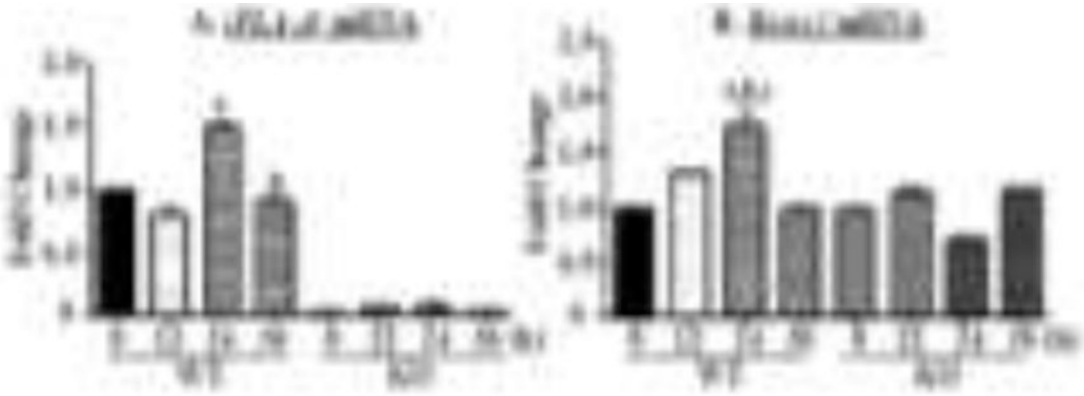

Fig. 4. Time course of *iPLA$_2\beta$* and *Runx2* induction in calvarial osteoblasts.

Calvarial osteoblasts prepared from WT and KO mice were cultured in Ost media for up to 36 h. At 12, 24, and 36 h the calvarial cells were processed for RT-qPCR analyses of *iPLA$_2\beta$* (*A*) and *Runx2* (*B*). *Hprt* was used as housekeeping control. Data are the means ± SEMs (3 independent measurements) of fold-changes relative to WT Con (undifferentiated) at 0 h (*A*) or relative to own Con at 0 h (*B*). (*A*, [a]significantly different from 0 h and 12 h, $p < 0.001$; [b]significantly different from 24 h, $p < 0.05$; *B*, [a]significantly different from 0 h, $p < 0.001$; [b]significantly different from 12 h, $p < 0.025$; [c]significantly different from 36 h, $p < 0.001$.)

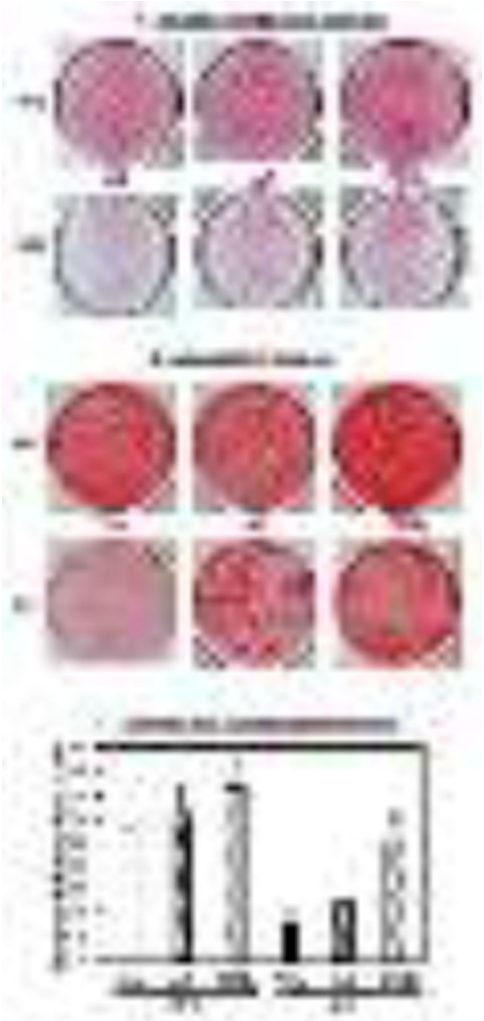

Fig. 5. Effects of AA and PGE_2 on mineralization in calvarial osteoblasts.

Calvarial osteoblasts of WT and $iPLA_2\beta$-deficient mice (KO) were harvested and cultured with osteogenic media with DMSO as vehicle (Veh), AA (10 μM), or PGE_2 (10 μM) supplementation at each media change for 7 days and stained for alkaline phosphatase (*A*) or alizarin red (*B*). *C*, Quantitation of alizarin red staining. Data are the means ± SEMs (3 independent measurements). ([a]Significantly different from WT Veh, $p < 0.05$; [b]significantly different from KO Veh, $p < 0.05$.)

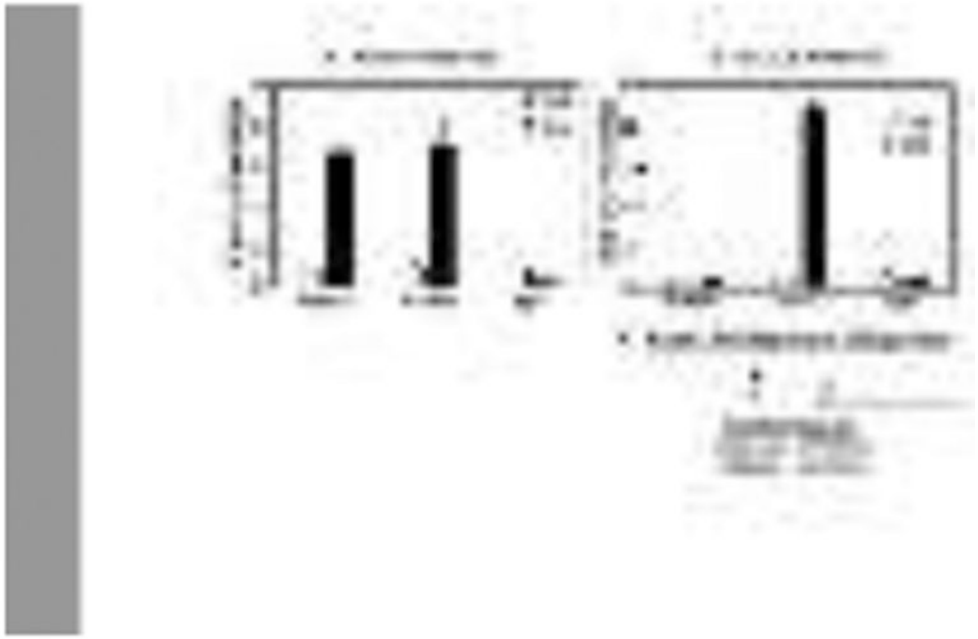

Fig. 6. Association of Runx2 with the *Runx2* and *Pla2g6* promoters during osteogenesis.

MC3T3-E1 cells were treated with Con or Ost media for 2 days. The ChIP analyses were performed with antibodies specific for Runx2, Ac-H3, or IgG and association with the *Runx2* (*A*) or *Pla2g6* (*B*) promoter regions analyzed by RT-qPCR. Data are representative analyses from 3-4 independent measurements. *C*, Schematic of mouse *Pla2g6* promoter and Runx2 consensus binding site. The mouse *Pla2g6* gene is located on chromosome 15 and spans the nucleotides from 79,170,428 to 79,212,295. The arrow indicates the start of transcription, which is denoted as +1. The Runx2 transcription factor bindings site is located at −961 bp relative to the transcription start site. For comparison, the consensus Runx2 binding site is shown and aligned with the Runx2 binding sites identified above.

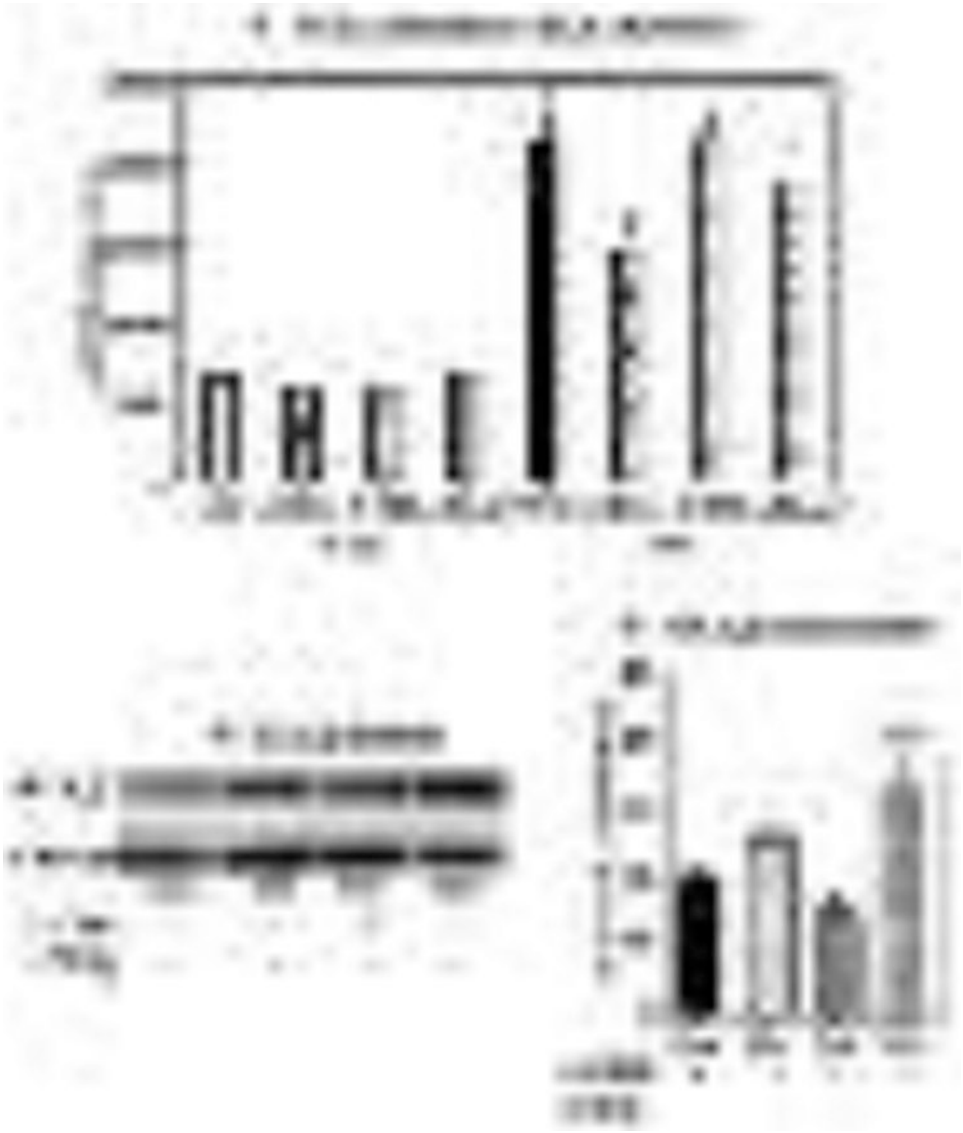

Fig. 7. Feedback regulation between PGE_2 and $iPLA_2\beta$.

A. PGE_2 production. MC3T3-E1 cells were cultured with Ost media in the presence of vehicle (DMSO), *S*-BEL (10 μM), *R*-BEL (10 μM), or CAY10502 (50 nM). Both *S*-BEL and *R*-BEL were present for only 1 h. After 48 h, the media were collected for PGE_2 EIA and the cell pellet for protein determination. The plotted data are means ± SEMs of pg PGE_2/mg protein (n=3-6). ([a]Significantly different from undifferentiated Con, $p < 0.001$; [b]significantly different from undifferentiated and differentiated Con, $p < 0.005$.) *B.* $iPLA_2\beta$ protein. The MC3T3-E1 cells were cultured with Con or Ost media in the absence or presence of *S*-BEL (10 μM) or PGE_2 (10 μM) for 48 h and processed for $iPLA_2\beta$ immunoblotting analyses (GAPDH, loading control). Representative immunoblots presented (from 3 independent experiments). *C.* Densitometry. $iPLA_2\beta$ band intensities, relative to corresponding loading control, are presented. ([a]Significantly different from Ost, $p < 0.025$; [b]significantly different from Ost, $p < 0.05$; [c]significantly different from Con, $p < 0.01$; [d]significantly different from *S*-BEL, $p < 0.025$.)

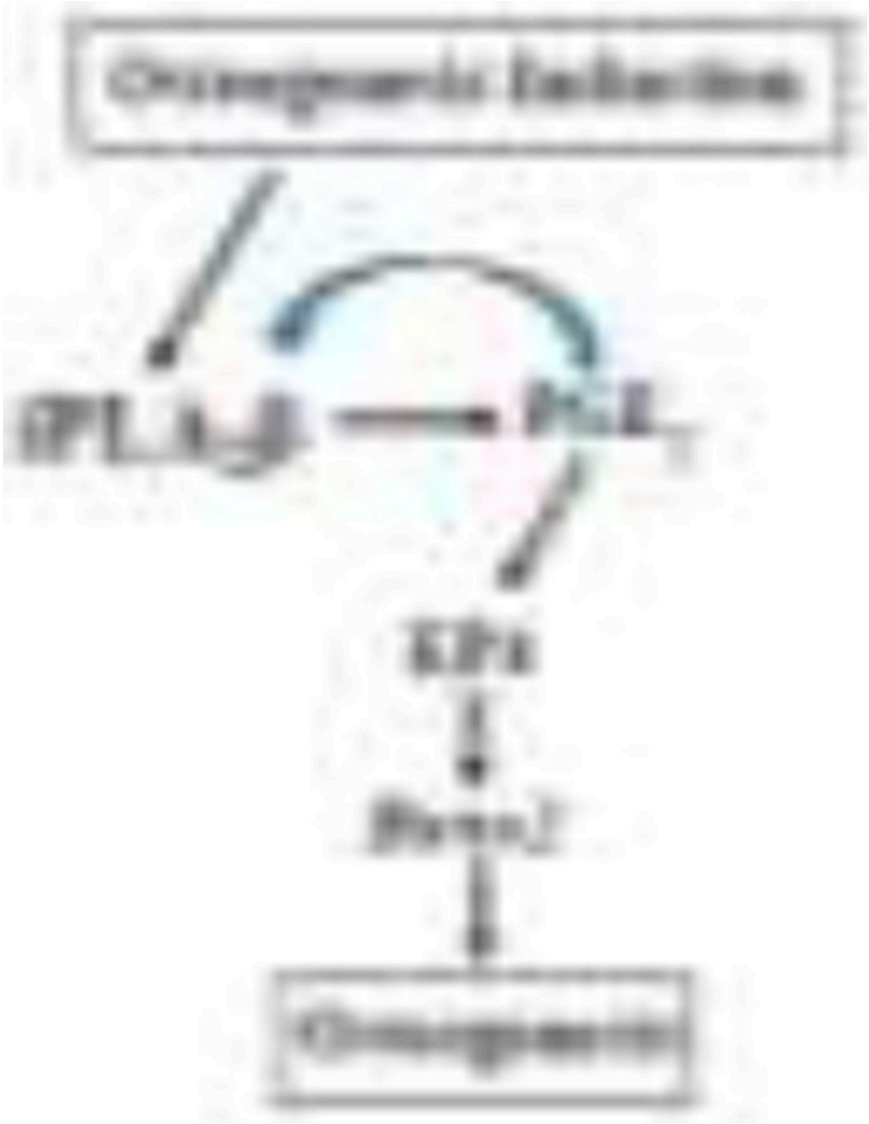

Fig. 8. Proposed model of iPLA$_2$β involvement osteogenesis.

We suggest that osteogenesis occurs via PGE_2 that is derived from iPLA$_2$β activation. We further posit that iPLA$_2$β-derived PGE_2 plays an important role in the regulation of not only Runx2 but, also of iPLA$_2$β.

Table 1.

Primers for Targets Analysed by RT-qPCR

Target	Sequence (5' to 3')	Product Size (bp)
Hprt	gcagcgtttctgagccattg	165
	taatcacgacgctgggactg	
iPLA$_2\beta$	tgtctctggggacaggaaa	264
	cagcactgcatcactgacct	
Runx2	atcagttcccaatggtacccg	215
	atcagttcccaatggtacccg	
Alpl	ttgtgccagagaaagagagaga	75
	gtttcagggcatttttcaaggt	
Bmp2	gggtggcgagagcttttcta	101
	ttcagagtggttgtcaatccg	

Table 2.

ChIP Primers for Targets Analysed by RT-qPCR

Target	Sequence (5' to 3')	Product Size (bp)
Pla2g6 Promoter	tacagggccacactggtcac	489
	atgggcagttcacatgatcg	
Runx2 Promoter	tgacgccatagtccctcctt	284
	ccaaccgagtcagtgagtgc	